

Experimental evaluation of impact ionization coefficients in $\text{Al}_x\text{Ga}_{1-x}\text{N}$ based avalanche photodiodes

Turgut Tut,^{a)} Mutlu Gokkavas, Bayram Butun, Serkan Butun, Erkin Ulker, and Ekmel Ozbay

Nanotechnology Research Center, Bilkent University, Bilkent, 06800 Ankara, Turkey; Department of Physics, Bilkent University, Bilkent, 06800 Ankara, Turkey; and Department of Electrical and Electronics Engineering, Bilkent University, Bilkent, 06800 Ankara, Turkey

(Received 8 August 2006; accepted 22 September 2006; published online 3 November 2006)

The authors report on the metal-organic chemical vapor deposition growth, fabrication, and characterization of high performance solar-blind avalanche photodetectors and the experimental evaluation of the impact ionization coefficients that are obtained from the photomultiplication data.

A Schottky barrier, suitable for back and front illuminations, is used to determine the impact ionization coefficients of electrons and holes in an AlGaN based avalanche photodiode. © 2006 American Institute of Physics. [DOI: 10.1063/1.2385216]

AlGaN based ultraviolet (UV) photodetectors with cut-off wavelengths smaller than 280 nm have proved their potential for solar-blind detection. They can be used in a number of civil and military applications such as missile warning and tracking systems, secure UV optical communication systems for space-to-space communication, ozone layer monitoring, biological agent, and gas detection. Due to their high responsivity (>600 A/W), high speed, and low dark current properties, photomultiplier tubes (PMTs) are frequently used for such applications. However, they are expensive, bulky, and require high operation voltages (usually >1 kV). In order to achieve solar-blind detection, PMTs should be integrated with complex and expensive filters. So, there is a certain need for high performance solid-state UV photodetectors that can be used to replace PMTs.¹ GaN (Refs. 2–8) and AlGaN (Refs. 9 and 10) based avalanche photodetectors (APDs) are suitable candidates for this purpose. In order to design a good GaN/AlGaN based APD, it is essential to know the electron and hole impact ionization coefficients over a wide range of E fields. In the literature there are theoretical works that report the impact ionization (II) coefficients in GaN/AlGaN,^{11–13} and only one experimental work reports the evaluation of II coefficients in GaN.¹⁴ However, there is no reported experimental work on the evaluation of II coefficients in AlGaN. In this letter, we report the experimental values of the II coefficients in $\text{Al}_{0.4}\text{Ga}_{0.6}\text{N}$ APDs.

The epitaxial structure of the avalanche photodetector is designed for back and front illuminations. In order to observe the avalanche effect, devices with low leakage and high breakdown are needed. The $\text{Al}_{0.4}\text{Ga}_{0.6}\text{N}$ absorption layer was used as a multiplication layer with $\lambda_c=276$ nm. The $\text{Al}_x\text{Ga}_{1-x}\text{N}$ epitaxial layers of our Schottky photodiode wafer were grown on a 2 in. double-side polished (0001) sapphire substrate using a metal-organic chemical vapor deposition (MOCVD) system that is located at Bilkent University Nanotechnology Research Center. A thin AlN nucleation layer was deposited first, and subsequently a $0.3 \mu\text{m}$ thick AlN buffer layer was deposited. Thereafter, a highly doped ($n^+=1.08 \times 10^{18} \text{ cm}^{-3}$) $0.3 \mu\text{m}$ thick $\text{Al}_{0.4}\text{Ga}_{0.6}\text{N}$

Ohmic contact layer was deposited, followed by a $0.2 \mu\text{m}$ thick $\text{Al}_{0.4}\text{Ga}_{0.6}\text{N}$ Schottky contact active layer with a relatively low doping ($n^-=1.45 \times 10^{17} \text{ cm}^{-3}$). The highly doped $\text{Al}_{0.4}\text{Ga}_{0.6}\text{N}$ layer was used for the Ohmic contact region in order to be compatible with the back illumination.

The samples were fabricated by using a five-step microwave-compatible fabrication process in a class-100 clean room environment.^{15–17} The dry etching was achieved via reactive ion etching (RIE) under CCl_2F_2 plasma, a 20 SCCM (SCCM denotes cubic centimeter per minute at STP) gas flow rate, and 200 W rf power. The etch rates for $\text{Al}_{0.4}\text{Ga}_{0.6}\text{N}$ layers were $200 \text{ \AA}/\text{min}$. The first mesa structures of the devices were formed via a RIE process, by etching all of the layers ($>0.8 \mu\text{m}$) down to the sapphire layer for better isolation. After an Ohmic etch of $\sim 0.3 \mu\text{m}$, Ti/Al ($100 \text{ \AA}/1000 \text{ \AA}$) contacts were deposited via thermal evaporation and left in an acetone solution for the lift-off process. The contacts were annealed at $700 \text{ }^\circ\text{C}$ for 60 s in a rapid thermal annealing system. The Schottky surface treatment was made with a diluted HCl solution. An $\sim 100 \text{ \AA}$ thick Au film was evaporated in order to form Au/AlGaN Schottky contacts. Then, a 200 nm thick Si_3N_4 was deposited via plasma enhanced chemical vapor deposition for passivation. Finally, $\sim 0.25 \mu\text{m}$ thick Ti/Au interconnect metal was deposited and lifted off to connect the Schottky layers to the coplanar waveguide transmission line pads.

The resultant devices had breakdown voltages higher than 60 V. To obtain better isolation, we etched down to the sapphire substrate, which enabled us to obtain low leakage current. The dark current for a $40 \mu\text{m}$ diameter device at 60 V was on the order of 1 nA. Figure 1 shows the dark current measurement with a low-level (on the order of femtoamperes) measurement setup. For reverse bias values below 15 V, the measured dark current was limited by the experimental setup and was approximately a few femtoamperes. The low dark current values proved the high growth quality of the AlGaN wafer with low dislocation densities. Hall measurements of the MOCVD grown samples showed that the active AlGaN layer had a Si doping concentration $N_d=1.45 \times 10^{17} \text{ cm}^{-3}$. Meanwhile, the Ohmic AlGaN layer had a Si doping concentration $N_d=1.08 \times 10^{18} \text{ cm}^{-3}$. Schottky barrier height of the fabricated photodetectors was

^{a)}Electronic mail: tturgut@fen.bilkent.edu.tr

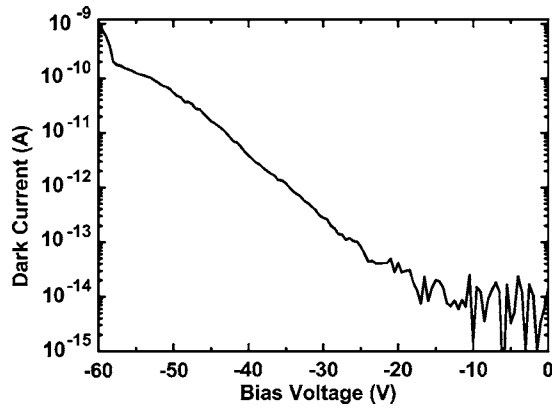


FIG. 1. Dark current of a 40 μm diameter photodetector.

calculated as 0.96 V by using the forward bias *I-V* data measured with a Keithley electrometer. To calculate the electric fields and depletion widths in the diode, we used one sided abrupt junction approximation.¹⁸

Figure 2 shows the quantum efficiency measurements of 150 μm diameter devices at 25 V. Under a 25 V reverse bias voltage, the device had a maximum quantum efficiency of 48% at 282 nm and of 10.64% at 290 nm with front and back illuminations, respectively. As can be seen in Fig. 2, the devices are responsive to photons with energies higher than 4.4 eV which qualified them to be solar blind. According to the quantum efficiency data, the photocurrent does not significantly increase after 20 V. Therefore, we set the unity gain at 20 V. We also had to adjust the light source intensity for front and back illuminated photomultiplication measurements. We used the Schottky barrier diode to achieve pure electron injection when illuminated on the Schottky metal side with photon energy higher than the Schottky barrier height (290 nm) and pure hole injection when illuminated on the sapphire side with energy higher than the band gap.¹⁹

Figure 3 shows the reverse bias voltage dependence of the electron and hole multiplication factors, M_n and M_p . The multiplication factors are the ratios of the multiplied photocurrents to the primary photocurrents injected. The impact ionization coefficients (Fig. 4) can be found from the multiplication factor data using the following formulation:²⁰⁻²²

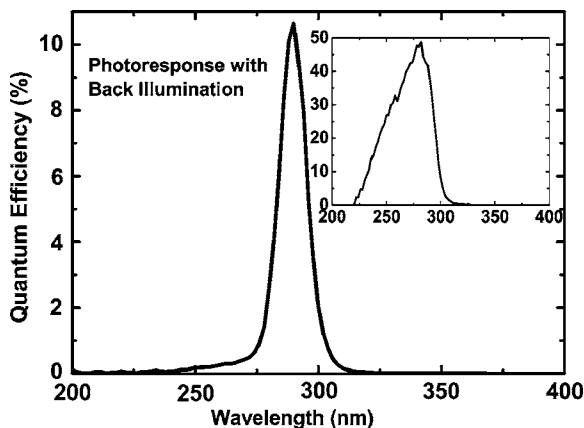


FIG. 2. Quantum efficiency with back illumination, in which the inset shows the results for front illumination.

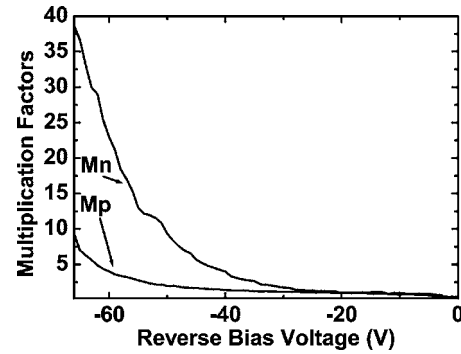


FIG. 3. M_n and M_p as a function of reverse bias voltage.

$$\beta(E_m) = \frac{2d}{W_0^2} \frac{1}{M_n M_p} \frac{dM_p}{dV} + \frac{M_p}{M_n} x \left(\alpha[E(d)] - \left\{ \alpha[E(d)] - \beta[E(d)] \right\} \frac{1}{M_p} \right), \quad (1)$$

$$\alpha(E_m) = \frac{2d}{W_0^2} \frac{1}{M_n} \frac{dM_n}{dV} + \alpha[E(d)] M_p - \beta(E_m) (M_n - 1), \quad (2)$$

$$W_0 = \left[\frac{2\varepsilon}{qN_d} \right]^{1/2}, \quad (3)$$

$$E(x) = \frac{qN_d}{\varepsilon} (W - x), \quad (4)$$

where E_m is the electric field near the Schottky contact metal for a certain applied bias voltage, and $E(d)$ is the electric field at the n^- - n^+ junction. $E(x)$ is the electric field at depth x from the Schottky metal and n^- layer interface, and V is the applied bias voltage across the device. Figure 4 shows the impact ionization coefficient data that were extracted from the multiplication factor data M_n and M_p . According to our calculations, α is larger than β for the range of electric field $0.78 < E < 1.88$ MV/cm. The ratio of α to β decreases as the electric field increases. The impact ionization coefficients can be fitted into an exponential form,

$$\alpha(E) = A_e \exp(-B_e/E), \quad (5)$$

$$\beta(E) = A_h \exp(-B_h/E), \quad (6)$$

where $A_e = 0.6 \times 10^6 \text{ cm}^{-1}$, $B_e = 3.6 \times 10^6 \text{ V/cm}$, $A_h = 3.4 \times 10^6 \text{ cm}^{-1}$, and $B_h = 7.9 \times 10^6 \text{ V/cm}$. The theoretical electron impact ionization coefficients (reported in Ref. 13) are

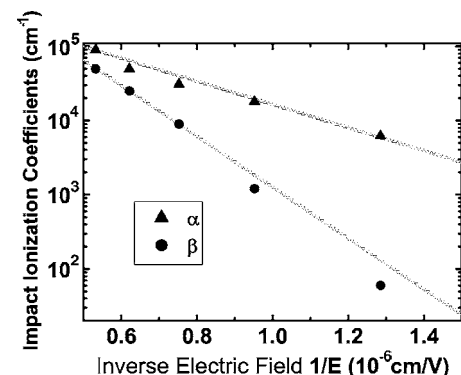


FIG. 4. Electron and hole impact ionization coefficients in $\text{Al}_{0.4}\text{Ga}_{0.6}\text{N}$.

significantly lower than our experimental impact ionization coefficients. We explain this discrepancy due to the lattice defects in the AlGaIn layers (which cause microplasmas) and the nonuniform E -field distribution which were not considered in the theoretical simulations of Ref. 13.

In summary, we present the MOCVD growth, fabrication, and characterization of AlGaIn based solar-blind APDs. The impact ionization coefficients for electrons and holes were evaluated from the photomultiplication measurements. Over the electric field range, $0.77 \text{ MV/cm} < E < 1.88 \text{ MV/cm}$, α is found to be larger than β .

This work is supported by the European Union under the projects EU-NOE-METAMORPHOSE, EU-NOE-PHOREMOST, and TUBITAK under Projects Nos. 104E090, 105E066, and 105A005. One of the authors (E.O.) also acknowledges partial support from the Turkish Academy of Sciences.

- ¹J. C. Campbell, S. Demiguel, F. Ma, A. Beck, X. Guo, S. Wang, X. Zheng, X. Li, J. D. Beck, M. A. Kinch, A. Huntington, L. A. Coldren, J. Decobert, and N. Tschertner, *IEEE J. Quantum Electron.* **10**, 777 (2004).
- ²K. A. McIntosh, R. J. Molnar, L. J. Mahoney, A. Lightfoot, M. W. Geis, K. M. Molvar, I. Melngailis, R. L. Aggarwal, W. D. Goodhue, S. S. Choi, D. L. Spears, and S. Verghese, *Appl. Phys. Lett.* **75**, 3485 (1999).
- ³J. C. Carrano, D. J. H. Lambert, C. J. Eiting, C. J. Collins, T. Li, S. Wang, B. Yang, A. L. Beck, R. D. Dupuis, and J. C. Campbell, *Appl. Phys. Lett.* **76**, 924 (2000).
- ⁴A. Osinsky, M. S. Shur, R. Gaska, and Q. Chen, *Electron. Lett.* **34**, 691 (1998).
- ⁵S. Verghese, K. A. McIntosh, R. J. Molnar, L. J. Mahoney, R. L. Aggarwal, M. W. Geis, K. M. Molvar, E. K. Duerr, and I. Melngailis,

- IEEE Electron Device Lett.* **48**, 502 (2001).
- ⁶K. A. McIntosh, R. J. Molnar, L. J. Mahoney, K. M. Molvar, N. Efremov, and S. Verghese, *Appl. Phys. Lett.* **76**, 3938 (2000).
- ⁷B. Yang, T. Li, K. Heng, C. Collins, S. Wang, J. C. Carrano, R. D. Dupuis, J. C. Campbell, M. J. Schurman, and I. T. Ferguson, *IEEE J. Quantum Electron.* **36**, 1389 (2000).
- ⁸J. B. Limb, D. Yoo, J. H. Ryou, W. Lee, S. C. Shen, R. D. Dupuis, M. L. Reed, C. J. Collins, M. Wraback, D. Hanser, E. Preble, N. M. Williams, and K. Evans, *Appl. Phys. Lett.* **89**, 011112 (2006).
- ⁹T. Tut, Serkan Butun, Bayram Butun, Mutlu Gokkavas, HongBo Yu, and E. Ozbay, *Appl. Phys. Lett.* **87**, 223502 (2005).
- ¹⁰R. McClintock, A. Yasan, K. Minder, P. Kung, and M. Razeghi, *Appl. Phys. Lett.* **87**, 241123 (2005).
- ¹¹Ismail H. Oguzman, Enrico Bellotti, Kevin F. Brennan, Jan Kolnik, Rong-ping Wang, and P. Paul Ruden, *J. Appl. Phys.* **81**, 7827 (1997).
- ¹²J. C. Cao and X. L. Lei, *Eur. Phys. J. B* **7**, 79 (1999).
- ¹³C. Bulutay, *Semicond. Sci. Technol.* **17**, L59 (2002).
- ¹⁴K. Kunihiro, K. Kasahara, Y. Takahashi, and Y. Ohno, *IEEE Electron Device Lett.* **20**, 608 (1999).
- ¹⁵N. Biyikli, T. Kartaloglu, O. Aytur, I. Kimukin, and E. Ozbay, *Appl. Phys. Lett.* **49**, 2838 (2001).
- ¹⁶E. Ozbay, N. Biyikli, I. Kimukin, T. Tut, T. Kartaloglu, and O. Aytur, *IEEE J. Sel. Top. Quantum Electron.* **10**, 742 (2004).
- ¹⁷T. Tut, N. Biyikli, I. Kimukin, T. Kartaloglu, O. Aytur, S. Unlu, and E. Ozbay, *Solid-State Electron.* **49**, 117 (2005).
- ¹⁸S. M. Sze, *Semiconductor Devices Physics and Technology* (John Wiley & Sons, New York, 1985), p. 78.
- ¹⁹M. H. Woods, W. C. Johnson, and M. A. Lampert, *Solid-State Electron.* **16**, 381 (1972).
- ²⁰N. Tabatabaie, V. M. Robbins, N. Pan, and G. E. Stillman, *Appl. Phys. Lett.* **46**, 182 (1985).
- ²¹S. L. Fu, T. P. Chin, M. C. Ho, C. W. Tu, and P. M. Asbeck, *Appl. Phys. Lett.* **66**, 3507 (1995).
- ²²B. K. Ng, J. P. David, S. A. Plimmer, M. Hopkinson, R. C. Tozer, and G. J. Rees, *Appl. Phys. Lett.* **77**, 4374 (2000).